Ab initio electron-structure calculations on the Nb/Ta multilayer system

1991 J. Phys.: Condens. Matter 3 3945

(http://iopscience.iop.org/0953-8984/3/22/007)

J. Phys.: Condens. Matter 3 (1991) 3945–3957. Printed in the UK

Ab initio electronic-structure calculations on the Nb/Ta multilayer system

H van Leuken†, A Lodder† and R A de Groot‡

† Faculteit Natuurkunde en Sterrenkunde, Vrije Universiteit De Boelelaan 1081, NL-1081 HV Amsterdam, The Netherlands

‡ Research Institute of Materials, Katholieke Universiteit Nijmegen, Toernooiveld 1, NL-6525 ED Nijmegen, The Netherlands

Received 23 November 1990

Abstract. *Ab initio* electronic-structure calculations are performed for Nb/Ta multilayers with small modulation wavelengths in the [100], [110] and [111] BCC modulation directions. The [110] modulated Nb/Ta multilayer with the smallest modulation wavelength was also calculated with an 8% increased modulation wavelength on the one hand, with an undisturbed structure but containing 50% interstitial hydrogen on the other hand, and with a combination of both.

The ease with which Nb/Ta multilayers can be grown in different modulation directions is understood from total energy calculations which show energy differences of less than 1 mRyd between the various directions. Further, it is found that interstitial hydrogen lowers the density of states at the Fermi level and that, but to a lesser extent, the lattice expansion on hydrogenation raises the density of states at the Fermi level. The net effect of a lowering of the density of states at the Fermi level is in agreement with the measured reduction of the superconducting critical temperature on hydrogenation.

1. Introduction

Since the first reports on the growth of metallic multilayers (ML), numerous metals have been combined into superlattices. However, the crystallographic quality that can be obtained in semiconductor superlattices has not been met in these structures. It might be possible to grow coherent metallic structures for small modulation wavelengths but, due to the lattice mismatch which is usually encountered between the constituent metals, incoherent structures are mostly realized. Because of strain and misfit dislocations, the interfaces between such mismatched metals are generally of a bad crystallographic quality. The ML of Nb and Ta form an exception to this. For this system almost perfect single-crystal superlattices are reported [1]. In these ML the common BCC lattice structure of Nb and Ta is essentially undisturbed and large coherency strains are avoided because of a lattice parameter difference smaller than 0.2%. Because the Nb/Ta ML are such a close realization of a perfect metallic superlattice they have been investigated intensively. In the present work we mainly want to concentrate on two experimental results for the Nb/Ta multilayer system.

(1) It has been found by Durbin *et al* [2] that Nb/Ta ML can be grown in different crystallographic directions. They reported on four single crystal superlattices grown

on chosen substrates, such that the modulation directions are [100], [110], [111] and [211]. In our calculations we will try to develop an understanding of this phenomenon on the basis of total energy calculations. Only the BCC [100], [110] and [111] directions and small modulation wavelengths are considered. This will be done in section 4.1. The density of states curves for these systems will be presented and discussed in section 4.2.

(2) Due to the history of the metals Nb and Ta as hydrogen absorbers the behaviour of their ML on hydrogenation has been studied extensively [3–7] in the last years. We focus on a small part of this work, namely on the superconducting properties of hydrogenated Nb/Ta superlattices as reported by Uher *et al* [6]. This will be done in section 4.3 where we calculate the density of states at the Fermi level for an Nb/Ta ML subject to lattice expansion and hydrogenation.

If one rules out interdiffusion, the Nb/Ta ML are a perfect system for band-structure calculations because no crystallographic assumptions have to be made. Despite this we could only find one previous band-structure calculation on this system [8]. In that work the general trends of the Nb/Ta [100] ML for a range of modulation wavelengths were studied by means of the surface-Green-function-matching method, employing an empirical tight-binding Hamiltonian. Self-consistency was not included. In our work we use the localized spherical-wave (LSW) method [9], an all-electron self-consistent-field method where the same approximations are employed as in the more familiar augmented spherical-wave method [10].

In sections 2 and 3 a description of the unit cells and the calculational parameters will be given respectively. Concluding remarks are made in section 5.

2. Unit cells

The unit cells of the Nb/Ta system are straightforwardly constructed by stacking the (100), (110) and (111) BCC planes. We only consider ML with equal numbers of planes for both metals, denoted as $n:n$, with a maximum of $n = 3$. Neither of the metallic parts needs to be deformed as both pure metals have the BCC structure and the same lattice parameter of 3.30 Å. (In fact they are 3.3003 Å for Nb and 3.3024 Å for Ta [2].) Furthermore, if one neglects interdiffusion [11], the cells can be chosen so that they contain only one atom per layer. Unit cells for the different modulation directions are depicted in figure 1. The 1:1 ML [111] cell is identical to the 1:1 [100] cell given in figure 1(a). This can be seen by realizing that the central atoms of the neighbouring cells constitute the two (111) Ta layers missing in this figure. In the 1:1 [100] cell, which has the CsCl structure and therefore can hardly be called a multilayer, the tetrahedral positions are marked on one face. These are formed by the atoms on the edges and two central atoms. Every face contains four tetrahedral positions. In the 1:1 [110] cell of figure 1(b), which is orthorhombic with dimensions $(a\sqrt{2}, a, a\sqrt{2})$, the primitive translation vectors are indicated. Increasing n amounts to stacking these units along the [100] and [110] directions and scaling of the c-axes by n. The 2:2 [111] cell depicted in figure 1(c) is trigonal or rhombohedral with lattice parameter $\frac{1}{2}a\sqrt{2}$ and an angle γ of 60°. The 3:3 [111] cell is described as trigonal with dimensions $(a\sqrt{2}, a\sqrt{2}, a\sqrt{3})$ of the hexagonal axes. The space groups (SG) of the structures discussed so far are given in table 1. Their description is based on the *International Tables* [12], to which the numbers in the column headed IT refer. Some remarks are in order. For the 2:2 system with direction [100] two choices for the origin are given in [12]. In this work origin 1

has been used. In addition, to describe the atomic positions in the trigonal system, it is possible to use hexagonal or rhombohedral axes. The use of the Wyckoff position 2*c* indicates that rhombohedral axes have been used. The orthorhombic systems are base-centred, i.e. they have the extra translations $(\frac{1}{2}, \frac{1}{2}, 0)$. The last row in table 1 gives information about the bulk metals Nb and Ta, which were calculated to serve as reference systems. For all structures in table 1 the radius R_{WS} of the ASA sphere, which is the Wigner–Seitz sphere of the underlying BCC structure, is the same, namely 1.625 Å.

Table 1. Nb/Ta ML crystallographic data.

ML	*n*	System	SG	IT	Wyckoff position Nb; Ta
[100]	1	Cubic (CsCl)	O_h^1	221	$1a; 1b$
	2	Tetragonal	D_{4h}^7	129	origin 1 : $2c, z = \frac{1}{8}; z = \frac{5}{8}$
	3	Tetragonal	D_{4h}^1	123	$1a, 2h, z = \frac{1}{6}; 1d, 2g, z = \frac{1}{3}$
[110]	1	Orthorhombic	D_{2h}^{19}	65	$2a; 2c$
	2	Orthorhombic	D_{2h}^{21}	67	$4g, z = \frac{1}{8}; z = \frac{5}{8}$
	3	Orthorhombic	D_{2h}^{19}	65	$2a, 4l, z = \frac{1}{6}; 2c, 4k, z = \frac{1}{3}$
[111]	2	Trigonal	D_{3d}^5	166	$2c, x = \frac{1}{8}; x = \frac{3}{8}$
	3	Trigonal	D_{3d}^3	164	$1a, 2d, z = \frac{1}{6}$; $1b, 2d, z = \frac{2}{3}$
Metal	—	BCC	O_h^9	229	$2a$

For the second part of this work, devoted to effects due to the presence of hydrogen, three deviations from the NbTa 1:1 [110] unit cell are calculated. The first one consists of a cell that has been elongated by 8% along the modulation direction. The space group remains unchanged but the *c*-axis is increased from 4.667 to 5.040 Å and R_{WS} to 1.667 Å.

The second cell, depicted in figure 2, consists of an undisturbed NbTa 1:1 [110] cell in which all six tetrahedral sites per metal are occupied by ASA spheres. Because the tetrahedral sites will become inequivalent when one of them is occupied by H the cell is described as triclinic with parameters $a = b = \frac{1}{2}\sqrt{3} \times 3.30$ Å and $c = \sqrt{2} \times 3.30$ Å and with an angle γ between the *a* and *b* axes of 70.53°. The cell contains 14 different classes. There is no longer any metal–metal ASA overlap, only overlap between the metal and tetrahedral sites and between the tetrahedral sites themselves. The R_{WS} are determined such that the overlap percentages, the percentage of volume of a sphere shared with one other sphere, are equal for the different overlaps of the spheres at the tetrahedral sites. With R_{WS} for the metallic positions chosen to be 51% larger than the radii of the spheres at the tetrahedral positions this overlap was 3% and the radii are 1.337 and 0.682 Å respectively. For comparison, the overlap between the metals in the undistorted cell is 2% of the metallic sphere volume and the maximal overlap in the distorted cell is 3%.

In the third cell both changes are combined. Because of the expansion of the *c*-axis the tetrahedral sites have become distorted. As a consequence there are now three different metal–tetrahedral-site overlap percentages and also three different overlap percentages between the tetrahedral spheres themselves. The relation between the sphere radii of the metals and the tetrahedral spheres is kept at 51% which raises the maximum overlap to 4%. The radius R_{WS} for the metallic positions now becomes 1.371 Å and for the tetrahedral positions 0.699 Å.

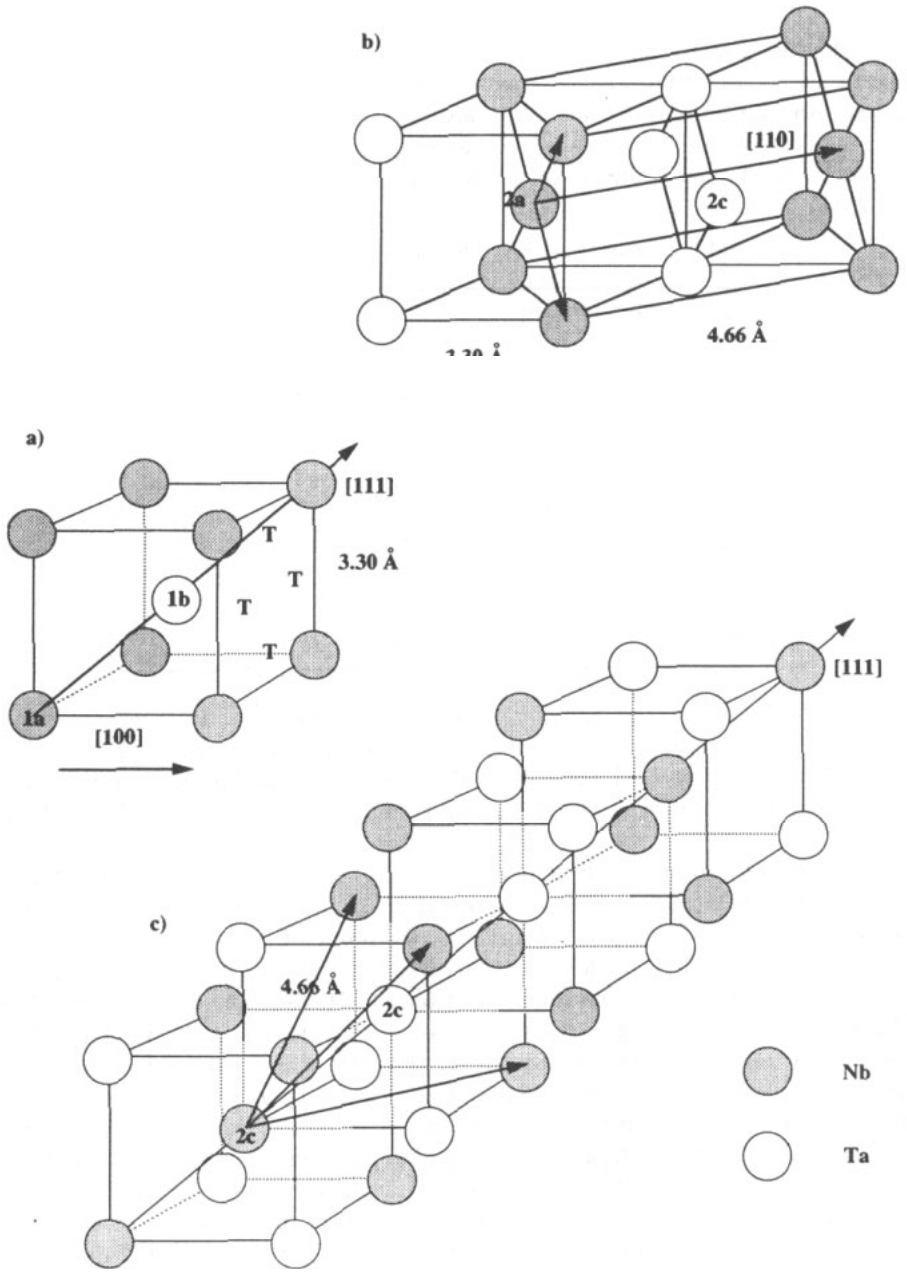

Figure 1. Unit cells for the Nb/Ta ML with Wyckoff positions for the atoms. The [100] modulated Nb/Ta 1:1 cell (*a*) also shows the tetrahedral sites for one face and the [111] modulation direction. The [110] modulated 1:1 cell (*b*) is base-centred orthorhombic with the primitive translations indicated. The two additional atoms complete the cube of (*a*). The 2:2 [111] cell (*c*) is rhombohedral. The translational vectors actually taken lie at $(-\frac{1}{8}, -\frac{1}{8}, -\frac{1}{8})$ from the indicated origin in order to have all the atoms of a kind in the same symmetry class. More atoms are drawn in for perspective.

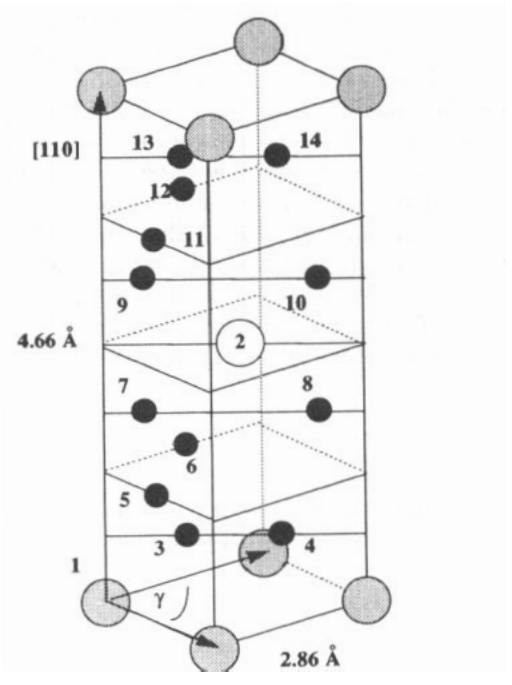

Figure 2. The basic NbTa 1:1 [110] cell for the metal–hydrogen calculations. The translational vectors are the same as in figure 1(*b*) but the *c*-axis is somewhat elongated for clarity. The angle γ is 70.53°. Calculations were performed with H at position 3 where three Nb atoms and one Ta atom form the tetrahedron and at position 5 with two Nb and two Ta atoms at the corners of the tetrahedron.

3. Calculations

Ab initio, self-consistent, localized spherical-wave (LSW) calculations [9] using a scalar-relativistic Hamiltonian have been carried out. We used local-density exchange-correlation potentials inside space filling, and therefore overlapping, spheres around the atomic constituents. The self-consistent calculations were carried out including all core electrons.

Iterations were performed with the k-points distributed uniformly in an irreducible part of the first Brillouin zone, corresponding to a volume of Brillouin zone per k-point of the order of 7×10^{-6} Å^{-3}. The density of k-points used for the bulk metals was twice as high and for the larger hydrogenated system about ten times smaller. Self-consistency was assumed when the changes in the local partial charges in each atomic sphere decreased to the order of 10^{-4}. Subsequently the partial densities of states were constructed by solving the Hamiltonian for a higher density of k-points, corresponding to a volume per k-point of the order of 3×10^{-6} Å^{-3} for the pure ML and 2×10^{-5} Å^{-3} for the hydrogenated systems. As sampling histograms, 300 channels with a width of 4.33 mRyd were used.

In the construction of the LSW basis [9], the spherical waves were augmented by solutions of the scalar-relativistic radial equations indicated by the atomic-like symbols 5s, 5p, 4d, and 6s, 6p, 5d corresponding to the valence levels of the parent metals Nb and Ta respectively. The internal l summation used to augment the central Hankel

function at surrounding atoms, was extended to $l = 3$, resulting in the use of 4f orbitals for Nb and 5f orbitals for Ta. The screening cluster consists of 8 nearest and 6 next-nearest neighbours, together with the central atom a total of 15 atoms, giving 126 degrees of freedom for screening the central Hankel functions. In the hydrogenated systems the functions 1s and 2p and 3d as an extension, were used for the hydrogen atom and the empty spheres. The cluster sizes are now bigger but there are smaller numbers of Hankel functions centred on the tetrahedral spheres. The metal atoms in the undistorted hydrogenated systems have clusters of 33 centres with 168 degrees of freedom and the tetrahedral positions have clusters of 31 centres with 140 degrees of freedom in the surrounding Hankel functions. The metal atoms in the distorted hydrogenated systems have clusters of 29 centres with 132 degrees of freedom and the tetrahedral positions have clusters of 35 centres with 156 degrees of freedom.

4. Results

In this section the results of the calculations are presented for the total energies (section 4.1) and the densities of states in the pure Nb/Ta systems (section 4.2) and the hydrogenated structures (section 4.3).

4.1. Total energies

In order to investigate the ease with which Nb/Ta superlattices can be grown in different orientations we have calculated total energies for three modulation directions with small wavelengths. The results given in Rydberg per Nb/Ta pair are presented in table 2. All numbers given have to be decreased with 38 822 Ryd to obtain the calculated values of the total energy.

Table 2. Total energies (Ryd per Nb/Ta pair), increased with 38 822 Ryd. Between parentheses the number of equal nearest neighbours are given.

n	[110]		[100]		[111]	
1	−0.2915	(4)	−0.2911	(0)	−0.2911	(0)
2	−0.2922	(6)	−0.2917	(4)	−0.2915	(4)
3	−0.2923	(8,6)	−0.2922	(8,4)	−0.2915	(6,3)

A first and important observation to be made is that the energies are about the same on a mRyd scale, even for the different numbers of layers n. This is a clear illustration of the similarity of the electronic properties of the constituent metals. Further one expects a relation with the experimental fact that these superlattices can be grown easily in different modulation directions, which is to be discussed later. However, small energy differences are seen along the rows of table 2 and also a decrease in energy on going to larger modulation wavelengths. We will first discuss these differences.

If an ML with a given underlying structure is grown in different directions only the type of neighbours of an atom is varied. In the Nb/Ta case, in which the underlying structure is the BCC structure, the different modulation directions for the ML can be ordered in groups of equal nearest neighbours (NN). In doing so and remembering that the total number of possible NN in a BCC structure is eight, we find the following. For

the 1:1 ML in the [100] direction no equal NN is present (see figure 1(*a*)) and the atoms in the [110] ML have four equal NN, which are ordered in a plane. For the 2:2 ML the atoms in both the [111] and [100] modulated structures have four equal NN, ordered tetrahedrally and pyramid-wise respectively. The [110] 2:2 ML atoms have six equal NN. In the 3:3 ML, there are two different layers of each metal. The central layer atoms have eight equal NN as in the bulk metals and four and six equal NN for the interface layer atoms in [100] and [110] respectively. However, in the [111] ML the central layer atoms have only six equal NN and the interface atoms have three equal NN.

We now have a scheme that runs across the rows and columns of table 2. If we order the energies in table 2 into groups corresponding to none, four and six or more equal NN, different levels arise. The 3:3 [111] ML can be placed in the group of four equal NN because it has an average number of 4.5 equal NN. The differences within the groups are of the order of 0.2 mRyd while between the groups the differences are about 0.4 mRyd. Smaller energy differences will not be discussed because they approach the accuracy of our results originating from the choice of the number of k-points and of the level of convergence. This classification reveals that essentially only the energy difference between the interaction of equal and distinct metals is of importance. In the Nb/Ta case this difference is of the order of tenths of mRyd. The question is whether this energy difference is important when growing ML of Nb and Ta. The actual growth process is a complicated phenomenon which can lead to various non-equilibrium structures. Note, however, that the substrate temperature of 780 °C, at which the Nb/Ta ML were grown [2], corresponds to a thermal energy k_BT of about 7 mRyd. The calculated energy differences lie well within this thermal energy which is available during the growth process. This implies that, if one orientation is kinetically stable with respect to the thermodynamically stable situation (the solid solution), all orientations will be kinetically stable and the substrate determines the growth direction.

It has already been noted that the energy decreases as n is increased, i.e. as the number of layers for each metal goes up. The metallic regions in the multilayer start to resemble the bulk metals or, equivalently, more atoms will have equal NN. According to this reasoning this energy decrease should be limited by the average energy of the bulk metals. However, this average energy is found to be −38 822.2920 Ryd, which is somewhat higher than the energy of the ML with more than four NN. This difference must be due to inaccuracies inherent to the various aspects of the method. Particularly one should keep in mind the approximation of using spherically averaged atomic potentials for atoms in different crystallographic symmetries. Since besides there are always inaccuracies due to the overlap of spheres one should be careful in interpreting total energies calculated by methods employing the ASA approximation. Still, the observed trends between the total energy and the number of equal NN is sufficiently significant and remains to be considered as a real effect.

4.2. Density of states

In this section the density of states (DOS) curves of the Nb/Ta ML system, together with the DOS curves of the bulk metals will be presented and discussed. These are displayed in figures 3 and 4. The DOS curves of the group V metals Nb and Ta are given in figures 3(*a*) and (*b*) respectively. It is observed that they are quite the same. This is what can be expected since, in addition to having the same number and kind of valence electrons, they both have the BCC structure and the same lattice parameter. Their common appearance consists of three sets of peaks, from −4 to −2 eV (for Ta

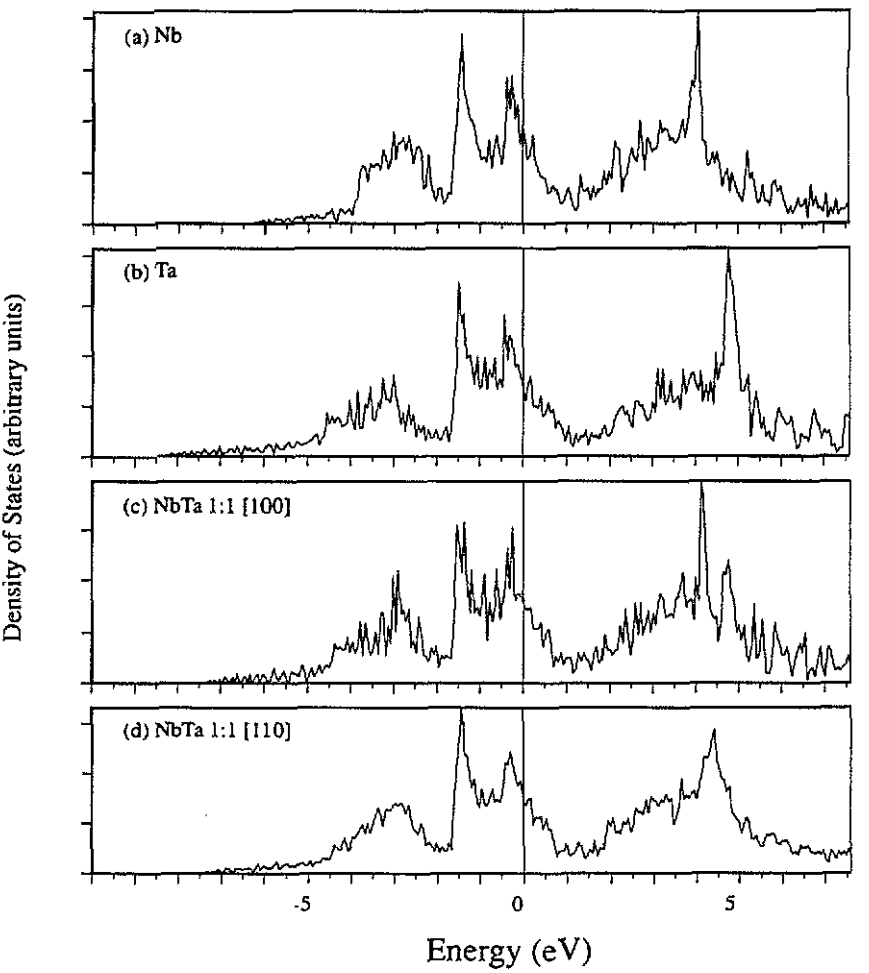

Figure 3. DOS curves for (*a*) bulk Nb, (*b*) bulk Ta and the ML of Nb/Ta 1:1 in the [100] modulation direction (*c*) and the [110] direction (*d*). The horizontal axis is in electron volts (eV) relative to the Fermi energy and the vertical axis is in arbitrary units.

this peak starts about 1 eV lower), from −1.5 to 1 eV and from 2 to 6 eV. There are some differences due to relativistic effects in that the heavier metal Ta has the onset of the (s) bands near −8.5 eV whereas they start at −6.5 eV in Nb. The most pronounced distinction is the position of a sharp peak above the Fermi level. This peak is just below 5 eV in Ta and about 1 eV lower in Nb.

The curves of the ML of Nb and Ta, in figures 3(*c*) and (*d*) and in figure 4, all have the same appearance. They share the same division in three sets of peaks as observed for the bulk metals and start with the band offset at the average value of the bulk metals of −7.5 eV. So we can restrict ourselves to discussing only differences within the sets of peaks. We start with the description of the [100] modulated 1:1 ML in figure 3(c). This ML, where every metal atom is surrounded by eight different atoms (see figure 1(*a*)), has the same local symmetry as the bulk metals. Because of the small energy difference between equal and distinct NN the splitting of the energy

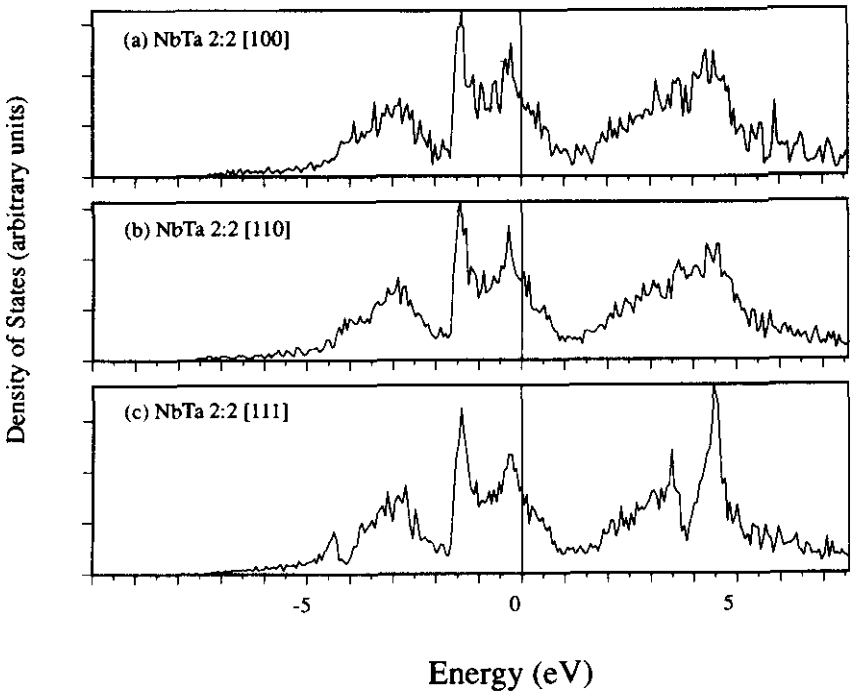

Figure 4. DOS results for the Nb/Ta 2:2 ML in the [100] (*a*), [110] (*b*) and the [111] (*c*) modulation directions. Axes are as figure 3.

levels of the bulk metals is left essentially undisturbed in this system. The resulting DOS curve looks like a superposition of the curves of bulk Nb and Ta although the peaks above E_F have moved closer together. The DOS curve of Nb/Ta 1:1 [110] in figure 3(*d*) looks like a smoothed version of figure 3(*c*). In particular the peaks above E_F have joined into one broad peak. To understand this feature one must take a look at figure 1(*b*). The atom labelled 2*a* has four equal neighbours in a rectangle in the (110) plane and four different neighbours in a similar rectangle in the $(1\bar{1}0)$ plane. Because of this different environment the energy levels that were degenerated in the [100] ML now split up and broaden.

The curves for the 2:2 (figure 4) and 3:3 ML consist of an average of contributions from different kinds of environments and look very much the same. Although there are some differences above the Fermi level, for instance in the 3:3 [111] DOS only the peak at 4.5 eV remains and the one at 3.5 eV is smeared out, the DOS curves of the 3:3 ML are not given. From figure 4 one clearly sees marked differences for the [111] ML compared with the other two directions. The differences in question are a dip at about −4 eV in the low energy structure for [111] and a dip in the region from 2 to 5 eV flanked by two sharp peaks, one at 3.5 eV and one at 4.5 eV. An atom in the 2:2 [111] ML has a typical surrounding in that it is positioned at the mutual centre of two tetrahedra, one formed by Nb atoms and the other formed by Ta atoms. Considering the positions and occupation numbers of the NN only, this situation (T_d) is similar to that of the parent metals (O_h) as far as the s, d electrons and their mutual interaction is concerned. In particular the high energy region turns out to be very sensitive to this effect.

Although no larger modulation wavelengths were considered it is clear that increasing the modulation wavelength will increase the bulk fraction. This will result in the reappearance in the DOS curves of the two separated sharp peaks above E_F.

4.3. Hydrogenated Nb/Ta multilayers

Uher *et al* [6] note that for hydrogenated Nb/Ta superlattices with increasing hydrogen concentration the superconducting transition temperature T_c is continuously depressed. It is suggested that the presence of hydrogen and the associated distortion of the cubic cell leads to a gradual suppression of the DOS at the Fermi level $N(E_F)$. In order to investigate the relationship of T_c with H concentration we calculated $N(E_F)$ for various deviations from the NbTa [110] system, by this simulating the system of interest. We restrict ourselves to the 1:1 ML, not only to save computer time, but also because in this cell the tetrahedral sites are formed by both constituting metals. On hydrogenating Nb/Ta ML there are two effects. The tetrahedral sites, six per metal, will become occupied gradually and due to this a volume expansion takes place. As a consequence of the epitaxial constraints imposed by the substrate during growth of the ML the volume expansion takes place only normal to the plane of the ML. The relationship between this one-dimensional volume expansion and hydrogen concentration c_H is given [6] by

$$\Delta V/V = \Delta a/a = 0.165 c_H \tag{1}$$

where a is the lattice parameter and c_H is expressed as the H-atom-to-metal-atom ratio. The proportionality constant 0.165 is the average value for the bulk metal–hydrogen systems of the ratio of the volume change per hydrogen atom and the volume of the host-metal atom. (If the hydrogen concentration becomes higher than a certain level hydrides will be formed. The hydrides can have different crystal structures from the host and they will not be considered here.)

Three different cells were calculated. A cell with an 8% increased c-axis, an undistorted cell but with 50% hydrogen and a cell with an 8% increased c-axis and also 50% hydrogen. According to equation (1) a 50% hydrogen concentration corresponds to 8.25% volume expansion. We took 8%, which was the maximum value of volume expansion reported in [6]. As already stated the tetrahedral sites are formed by both constituting metals but they are not all equivalent. We note that there are three different tetrahedral sites for H to occupy (see figure 2). Position 3, where there are three Nb atoms and one Ta atom at the corners of the tetrahedron, position 5 with two Nb and two Ta atoms and position 7 with one Nb and three Ta atoms. The other tetrahedral positions in this figure are symmetry related to these. The hydrogenated ML were calculated with H at position 5, the most symmetrical position, which has the relative coordinates $(\frac{1}{2}, 0, \frac{1}{4})$. To investigate the dependence of the results on the H position, the calculations were repeated with H at position 3 $(\frac{3}{8}, \frac{3}{8}, \frac{1}{8})$. Position 7 was not considered. The following discussion will be based on the systems with hydrogen at position 5.

The DOS curves for the different systems are given in figures 5(b) to (d). For comparison in figure 5(a) the already discussed DOS of the 1:1 [110] ML is given (see figure 3(d)). The DOS at the Fermi energy is determined from the DOS histogram by linearly interpolating between the $N(E)$ values at the two adjacent histogram channel energies. The values in arbitrary units are given in table 3. The results for the calculations with H at position 3 in figure 2 are given between parentheses.

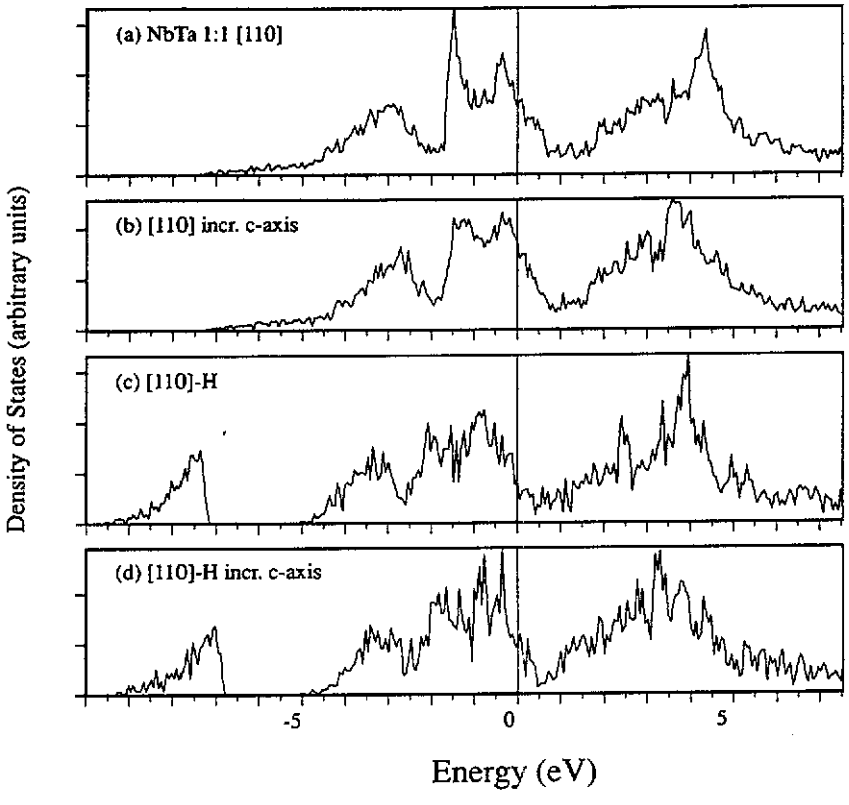

Figure 5. DOS for Nb/Ta 1:1 [110] as in figure 3(*d*), according to the unit cell of figure 1(*b*). This system was also calculated for a cell with an 8% increased *c*-axis (*b*), for the cell of figure 2 containing 50% hydrogen at position 5 and for a combined cell with an 8% increased *c*-axis and 50% hydrogen at position 5(*d*). Axes are as in figure 3.

Table 3. DOS at the Fermi level in arbitrary units. Between parentheses the results of H at position 3.

ML	$N(E_F)$	
[110] undistorted	32.3	
[110] incr. *c*-axis	41.4	
[110]-H	17.7	(19.4)
[110]-H incr. *c*-axis	24.0	(21.8)

It must be noted that these calculations have different levels of approximation with respect to the atomic spheres, because cells are compared with different kinds of ASA overlaps. However, in these calculations, which were performed in search for trends, $N(E_F)$ is less sensitive to this because the DOS histograms are based on 4.33 mRyd channels.

We will explain the densities of states at the Fermi level by discussing the DOS curves of the different cells that were calculated. The first case is where the length of the *c*-axis is increased. This amounts to an increase of the distance between the

(110) planes but leaving the in-plane distances between atoms of a kind fixed. If interatomic distances are increased, the wavefunction overlap decreases and the bands become narrower. This explains the shift of the peak which is in 1:1 [110] at 4.5 eV (figure 5(*a*)) to below 4 eV if the *c*-axis is increased (figure 5(*b*)). Because of the asymmetric volume expansion, only part of the peaks respond in this way, while other peaks remain unchanged. This explains the second observation if the cell is one-dimensionally expanded, namely the flattening of the structure from −1.5 to about 1 eV. A part of the high peaks in this region move together, lowering the maxima and filling the minima. Narrowing the peaks, while the integral over the DOS must remain constant, necessarily increases the DOS. The $N(E_F)$ of 1:1 [110] is increased from 32.3 to 41.4 by expanding the *c*-axis.

Introducing hydrogen into 1:1 [110], without lattice expansion, gives a completely different picture. The most striking result is the appearance of the structure in the region from about −9.5 to about −7.1 eV. This region contains exactly two electrons according to the integrated DOS. One electron is introduced with the proton and one electron must have come from previously occupied Nb/Ta states as seen in figure 5(*a*). One striking contribution to the latter apparently originates from the free-electron-like *s*-character states at low energies (−5, −7 eV). In the hydrogenated ML system these states have completely disappeared and an energy gap between the new structure at −7 eV and the onset of the metal d-states at −5 eV occurs. This is a fingerprint of the distinction between *compound formation* rather than alloy formation as is encountered in, for example, the unhydrogenated ML. As for effects on the DOS around E_F we remark that figure 5(*a*) can be compared with figure 5(*c*) by shifting the latter about 0.4 eV to the right. In this way the three broader features in figure 5(*a*) coincide with those in figure 5(*c*). Although there are some changes in the details of the features due to the new situation, we now can interpret the effect of hydrogenation as shifting the Fermi level to higher energies. In Nb and Ta, where the DOS has a decreasing tendency in a region of about 1.5 eV above the Fermi level, hydrogenation will correspond to a lowering of the DOS at the Fermi energy. The DOS at the Fermi energy has decreased from 32.3 in the pure ML to a value of 17.7 on hydrogenation. Note that in this work we are considering hydrogenation as occupying tetrahedral sites only and that no separate phases are considered.

For the two structures representing the decoupled effects of hydrogenation we have observed a decrease of $N(E_F)$ solely due to the introduction of hydrogen and an increase due to the lattice expansion, the latter being a smaller effect. The final curve to discuss combines the previous two aspects. Because it is not completely clear how the effects couple, the combined effect was calculated, leading to the DOS curve given in figure 5(*d*). Compared with figure 5(*c*) we see the same effect as already discussed for figure 5(*b*). We note that the largest peak above the Fermi level has lowered its energy by about 1 eV, the same amount as in figure 5(*b*) and that also the split-off states at the low energy end of the DOS curve have shifted towards the Fermi level. The DOS at the Fermi level is increased from 17.7 for the hydrogenated system without lattice expansion to 24.0 on expanding the *c*-axis. One can conclude from this, at least in a qualitative way, that the effects of hydrogenation and lattice expansion can be added with respect to the DOS at the Fermi level. The same observation can be made for H at position 3 in figure 2, although the effect is smaller in this case. More importantly, the DOS at the Fermi level is significantly lower in the hydrogenated ML system than in the pure ML system. Concentrating on $N(E_F)$ alone, according to the BCS theory this will result in lower T_cs for the hydrogenated ML than for the pure ML,

which is in agreement with experiment [6].

5. Conclusions

The essence of changing the orientation of the growth direction for metallic multilayers, keeping the underlying structure the same, is that the nearest neighbour environment of the atoms is changed. In the Nb/Ta multilayer system the energy differences between various nearest neighbour situations were identified and found to be less than 1 mRyd. This relative independence of energy can be seen as an explanation for the ease with which Nb/Ta multilayers can be grown in chosen orientations. Regarding the hydrogenation of Nb/Ta multilayers as occupying tetrahedral sites by H, we find that the only cause of the observed lowering of the superconducting transition temperature is the hydrogen insertion. The accompanying volume expansion raises the density of states at the Fermi energy, by that opposing the effect of hydrogen insertion. Due to the similarity of the density of states curves of Nb and Ta XPS spectra of their multilayers will probably be indistinguishable. The unoccupied states show more distinction, but only for the smallest modulation wavelengths. Interdiffusion may diminish these effects however. For larger modulation wavelengths than those considered in this work, the bulk metallic peaks will reappear.

Acknowledgment

This work is part of the research program of the 'Stichting voor Fundamenteel Onderzoek der Materie (FOM)', which is financially supported by the 'Nederlandse Organisatie voor Wetenschappelijk Onderzoek (NWO)'.

References

[1] Durbin S M, Cunningham J E, Mochel M E and Flynn C P 1981 *J. Phys. F: Met. Phys.* **11** L223
[2] Durbin S M, Cunningham J E and Flynn C P 1982 *J. Phys. F: Met. Phys.* **12** L75
[3] Miceli P F, Zabel H and Cunningham J E 1985 *Phys. Rev. Lett.* **54** 917
[4] Miceli P F and Zabel H 1987 *Phys. Rev. Lett.* **59** 1224
[5] Miceli P F and Zabel H 1987 *Superlatt. Microstruct.* **3** 519
[6] Uher C, Cohn J L, Miceli P F and Zabel H 1987 *Phys. Rev.* B **36** 815
[7] Miceli P F and Zabel H 1989 *Z. Phys.* B **74** 457
[8] Velasco V R, Baquero R, Brito-Orta R A and Garcia-Moliner F 1989 *J. Phys.: Condens. Matter* **1** 6413
[9] van Leuken H, Lodder A, Czyżyk M T, Springelkamp F and de Groot R A 1990 *Phys. Rev.* B **41** 5613
[10] Williams A R, Kübler J and Gelatt C D Jr 1979 *Phys. Rev.* B **19** 6094
[11] Durbin S M, Cunningham J E and Flynn C P 1987 *J. Phys. F: Met. Phys.* **17** L59
[12] Hahn T 1983 *International Tables for Crystallography Vol. A: Space Group Symmetry* (Dordrecht: Reidel)